LATTICE PARAMETER MEASUREMENTS IN ZED-2

by

R.E. Green and C.B. Bigham

A paper to be presented at the

I.A.E.A. Symposium on Exponential and Critical Experiments

to be held 2-6 September 1963 at Amsterdam, Netherlands

LATTICE PARAMETER MEASUREMENTS IN ZED-2

by

R.E. Green and C.B. Bigham

A B S T R A C T

Experiments have been done in the ZED-2 reactor to determine lattice parameters for fuel assemblies which closely resemble the fuel channels of the CANDU power reactor. The experimental fuel consisted of 19-rod clusters of 1.421 cm diameter, zircaloy-clad UO_2 of density 10.45 gm/cm^3 housed in double-walled tube assemblies to simulate the pressure and calandria tubes of the power reactor. Measurements were made in hexagonal lattices for several pitches in the range 18-36 cm with three different materials filling the coolant spaces of the fuel assemblies; viz., D_2O, air (i.e. void) and an organic liquid called HB-40, which has the chemical formula $C_{18}H_{22.0}$. The moderator was in all cases D_2O. The following quantities were determined:

bucklings which were derived from macroscopic flux distributions and reactivity measurements,

microscopic neutron activation distributions from which the average neutron densities in the various cell materials were deduced,

the epithermal neutron spectrum index r,

the effective neutron temperature T_n,

fast fission ratios, and

initial conversion ratios.

AECL-1814

A paper to be presented at the
I.A.E.A. Symposium on Exponential and Critical Experiments
to be held 2-6 September 1963 at Amsterdam, Netherlands

Table of Contents

Introduction

The ZED-2 reactor (1) at Chalk River is a D_2O-moderated, zero-energy, critical facility in which experiments are done to determine the parameters of lattices of fuel assemblies which are possible contenders as fuel for nuclear power stations. In addition to obtaining information for a particular lattice arrangement of interest, measurements are made for various lattice arrangements, i.e., different lattice pitches and with different fuel conditions, e.g., different coolant materials, to provide a broad experimental background for the lattice recipes used by the designers of future power reactors. Since ZED-2 first went into operation in September 1960, detailed lattice parameter measurements have been made for lattices of fuel assemblies which are similar to the fuel channels of the NPD and CANDU power reactors. Experimental results for lattices of NPD type 7-rod UO_2 fuel bundles were presented at the I.A.E.A. Panel Meeting on Heavy Water Lattices in Vienna in February, 1963 (2). This paper describes the results that have been obtained for lattices of CANDU type 19-rod UO_2 fuel bundles.

Description of Fuel and Lattice Arrangements

Fig. 1 is a cross-sectional view of one of the fuel assemblies used in the experiments. The fuel is in the form of bundles each consisting of 19 pencils of UO_2 having a diameter of 1.421 cm, and a density of 10.45 gm/cm^3. Each pencil was sheathed in 0.454 mm thick zircaloy-2. More details of the fuel bundles are shown in Fig. 2. Each assembly contained six bundles. The main differences between

the experimental fuel assemblies and the actual CANDU fuel channels are different bundle end-plates, and the fact that the experimental pressure and calandria tubes were Al whereas in CANDU they are zircaloy-2 and zircaloy-4 respectively. However, the thickness of the Al pressure tube was chosen to give the same thermal neutron absorption as the actual pressure tube. Seven assemblies were also available having zircaloy-2 pressure tubes (but Al calandria tubes) and these were used to determine the material bucklings of lattices of assemblies with zircaloy pressure tubes. The physical details of the experimental fuel assemblies are listed in Table I. Note that the bundle end region is defined as that region lying between the UO_2 in adjacent bundles and extending radially to the inside surface of the pressure tube.

Experiments have been done with three different materials in the coolant space, viz., D_2O of moderator purity, air (i.e., void) and an organic liquid, HB-40, which is a yellowish liquid having a formula of $C_{18}H_{22.0}$, a density of 1.00 gm/cm^3 at 25°C, and a temperature coefficient of density of -0.065% /°C in the range 0°C to 300°C. In the D_2O-cooled lattices the D_2O entered the coolant space from the moderator region through holes in the bottoms of the assemblies. The air-cooled lattices were obtained by excluding the D_2O coolant with He gas; each assembly was made airtight and fitted at the top with plastic tubing which was connected via a manifold to a cylinder of helium gas located outside the reactor. The D_2O was forced from the coolant space into the moderator region. The organic HB-40 coolant was sealed

Table I: Details of ZED-2 Experimental Fuel Assemblies

Detail		7-rod Bundles*	19-rod Bundles** Type 1	19-rod Bundles** Type 2
Bundle Length	cm	47.31	49.38	49.38
UO_2 Fuel:				
Length per bundle	cm	45.72	47.73	47.73
Diameter	cm	2.400	1.421	1.421
Density	gm/cm^3	10.20	10.45	10.45
Sheath Spacing	mm	1.27	1.27	1.27
Fuel Sheath:				
Material		Al	ZR-2†	ZR-2
I.D.	cm	2.438	1.431	1.431
Wall Thickness	mm	0.508	0.454	0.454
Pressure Tube:				
Material		Al	Al	ZR-2
I.D.	cm	8.255	8.255	8.283
Wall Thickness	mm	0.89	2.67	4.28
Calandria Tube:				
Material			Al	Al
I.D.	cm	-	10.160	10.160
Wall Thickness	mm	-	1.42	1.42
Bundle End Region:				
Gap Between UO_2	cm	1.59	1.65	1.65
Volume of Sheath Material	cm^3	59.52	23.48	23.48
Volume of Air	cm^3	5.23	6.36	6.36
Volume of Coolant	cm^3	20.24	58.52	59.10

* The centres of the six outer rods lie on a 5.33 cm diameter circle.

** The 19 rods are in a circular array; one rod on the axis, six on a 3.30 cm diameter circle and twelve on a 6.38 cm diameter circle.

† ZR-2 = Zircaloy-2

inside the coolant space, and thus isolated from the moderator.

Measurements were made in triangular lattices for a range of lattice pitches, 18-36 cm for the D_2O and air-cooled lattices and 18-28 cm for the organic-cooled lattices. All measurements were made in arrays of 55 assemblies. For the D_2O and air-cooled lattices at pitches greater than 21 cm only 55 fuel assemblies were required. Extra reactivity was required for all of the organic-cooled lattices and for the D_2O and air-cooled ones at 21 cm pitch and smaller. This was provided by adding six of the assemblies with zircaloy pressure tubes and/or ZEEP rods (3) or NPD type 7-rod UO_2 cluster assemblies (1) around the outside of the core. A typical lattice arrangement is shown in Fig. 3, viz., the 21 cm D_2O-cooled lattice arrangement.

Experimental Techniques

The program of measurements was aimed at the determination of the following lattice parameters for several different lattice pitches with each of the three coolants: the material buckling B^2, the microscopic neutron density distribution throughout the lattice cell, the initial conversion ratio γ_o, the fast fission ratio δ; and also the neutron spectrum parameters: the epithermal spectrum index r and the effective neutron temperature T_n. The experimental techniques used to determine them will now be described.

1. Bucklings

The bucklings were determined from flux distribution measurements made with Mn (11% Ni) foils mounted in thin Al thimbles

which were placed at cell boundary positions throughout the core. The resulting flux distributions well-removed from the core boundaries (the radial positions used in the analysis are shown in Fig. 3) were fitted by least squares to J_o or I_o Bessel and cosine functions to determine the radial and axial bucklings respectively. (The radial flux distribution was of the I_o form in some low-buckling, tight lattices where a large driving region was used and there was a net flow of neutrons into the core from the driver region; in these cases the axial geometric buckling exceeds the material buckling.) Since the fuel is in the form of bundles, "flux peaking" at the elevations of the bundle ends was observed particularly at tight spacings. The measured fluxes at the bundle end locations were omitted from the axial fitting.

Material bucklings were also obtained for lattices of D_2O-cooled assemblies having zircaloy-2 pressure tubes by measuring the reactivity effect of replacing the central seven assemblies having Al pressure tubes with ones having zircaloy pressure tubes. The procedure used was to measure the critical heights for three different reactor configurations, viz.,

(i) the normal unperturbed reactor containing a core of 55 fuel assemblies with Al pressure tubes

(ii) the normal core ((i) above) but with a 2.54 mm diameter full length Co wire located at the boundary of the central cell, and

(iii) the normal lattice with the seven central fuel assemblies of the core replaced by ones having zircaloy-2 pressure tubes.

The changes in geometric buckling, ΔB^2, of the unperturbed lattice required to compensate for the perturbations were assumed to be given by,

$$\Delta B^2 = F(h)\ \pi^2 \left[\frac{1}{(h+\Delta h)^2} - \frac{1}{h^2} \right] \qquad (1)$$

where Δh is the change in height required to keep the reactor critical when the perturbation is made,

h is the extrapolated height of the unperturbed reactor, and

$F(h)$ is a factor which allows for the dependence of the radial leakage upon critical height. This is a reflector effect which depends upon the height h and the reflector properties and is known from other experiments to vary from 1.0 to 1.5 for the lattices studied here.

Using one-group statistical weight theory it can be shown that,

$$B^2_{ZR} = B^2_{Al} + \frac{\Delta B^2_{ZR}}{\Delta B^2_{Co}} \frac{W_1}{W_7} (B^2_{Co} - B^2_{Al}) \qquad (2)$$

where ΔB^2_{Co}, ΔB^2_{ZR} are the observed buckling changes for the Co wire and the seven-assembly fuel replacement respectively, obtained using equation (1),

B^2_{ZR} is the required material buckling of the lattice of fuel assemblies with zircaloy-2 pressure tubes,

B^2_{Al} is the material buckling of the lattice of fuel assemblies with Al pressure tubes,

B^2_{Co} is the material buckling of a lattice of fuel assemblies with Al pressure tubes and also a full length 2.54 mm diameter Co wire located at the boundary of each cell, and

W_1, W_7 are the statistical weights of the central cell and the central seven cells, respectively, of the unperturbed reactor.

$$\frac{W_1}{W_7} = \frac{\int_1 \phi^2 dV}{\int_7 \phi^2 dV} \qquad (3)$$

where $\int_1, \int_7$ are integrations over the central cell and central seven cells respectively, and

ϕ is assumed to be given by

$$\phi = J_o(\lambda r)\cos(\beta z) \qquad (4)$$

where $\lambda^2 = B^2_{Al} - \beta^2$ and

$\beta = \pi/h$.

Here only the radial dependence of ϕ is required since the perturbations are all full-length. All quantities in equation (2) except B^2_{Co} are known from measured flux distributions and critical heights. $(B^2_{Co} - B^2_{Al})$ was calculated using the known cross section of Co, measured cell flux distributions and the flux depression factor for the Co wire which was measured separately. In making

this calculation η and ϵ were assumed constant but the effect of the presence of the Co on all other parameters was included.

2. Microscopic Neutron Density Distributions

Neutron activation distributions were measured throughout central lattice cells with ~0.10 mm thick Mn-Ni foils placed between fuel pellets and 0.51 mm diameter Mn-Ni wires located in holes drilled ultrasonically in the fuel pellets and at various positions in the coolant region and moderator. These measurements were made in a special short fuel assembly which replaced the normal central fuel assembly and which contained only three fuel bundles, the middle one of which was the experimental bundle. The measurements were made near the middle (axially) of this fuel bundle, well away from the end effects.

The total activities obtained were corrected for the macroscopic flux variation across the cell and for Mn resonance activation using the measured neutron spectrum parameters (see below) to arrive at the total neutron density distribution throughout the lattice cell. Since the total Mn activation is proportional to

$$n\sigma_o \left(G_t g + G_r s_o r \sqrt{T_n/T_o}\right)$$

where n is the total neutron density,

σ_o is the 2200 m/s cross section of Mn,

G_t, G_r are the thermal and resonance self-shielding factors for the detectors,

$s_o \equiv s\sqrt{T_o/T_n}$ and

g,r and s are the well known parameters defined by Westcott et al. (4).

The relative neutron density distribution is obtained by dividing the measured activities by the appropriate $(G_t g + G_r s_o\ r\sqrt{T_n/T_o}\ )$ factor using the measured values of $r\sqrt{T_n/T_o}$. G_t values were calculated, g was taken as 1.000 for Mn and $G_r s_o$ values were measured in separate Cd ratio experiments using thin Au foils as a standard. Graphical integration is used to determine average neutron densities in the various cell materials.

3. Neutron Spectrum Parameters

Measurements of the epithermal neutron spectrum parameter r, and the effective neutron temperature T_n (a measure of the spectral hardening) were made in the fuel, at a cell boundary position in the moderator and on the outer surface of the calandria tube. The technique used has been described in detail by Bigham et al. (5). Thin In-Al and Lu-Mn-Al foils were irradiated together at several positions inside the fuel cluster and in the moderator of the central cell and also at a reference position, either in the D_2O reflector outside the core or in the graphite reflector below the calandria floor. Once the specific activities of the In, Mn and Lu-176 detectors have been determined, the values of r and T_n are deduced using the following expressions;

$$\frac{(A_{In}/A_{Mn})_x}{(A_{In}/A_{Mn})_o} = \left[\frac{(G_t g + (r\sqrt{T_n/T_o})_x G_r s_o)_{In}}{(G_t g + (r\sqrt{T_n/T_o})_x G_r s_o)_{Mn}}\right]\left[\frac{(G_t g + (r\sqrt{T_n/T_o})_o G_r s_o)_{Mn}}{(G_t g + (r\sqrt{T_n/T_o})_o G_r s_o)_{In}}\right] \quad (5)$$

$$\frac{(A_{Lu\text{-}176}/A_{Mn})_x}{(A_{Lu\text{-}176}/A_{Mn})_o} = \left[\frac{(G_t g_x + (r\sqrt{T_n/T_o})_x G_r s_o)_{Lu\text{-}176}}{(G_t g + (r\sqrt{T_n/T_o})_x G_r s_o)_{Mn}}\right]\left[\frac{(G_t g + (r\sqrt{T_n/T_o})_o G_r s_o)_{Mn}}{(G_t g_o + (r\sqrt{T_n/T_o})_o G_r s_o)_{Lu\text{-}176}}\right] \quad (6)$$

where A is the specific activity,

x refers to the position in the test cell, and

o refers to the reflector reference position.

The value of $(r\sqrt{T_n/T_o})_o$ is determined by measuring the Cd ratio for thin In-Al foils at this position; $(r\sqrt{T_n/T_o})_o$ is small so that the uncertainty in its measurement introduces a negligible error in the determination of $(r\sqrt{T_n/T_o})_x$. Values of $G_r s_o$ for the detectors are known from Cd ratio measurements and are based on the value $s_o = 18.8$ for In suggested by Bigham et al. (5). G_t values are calculated and g values are taken from Westcott (6). Thus values of $r\sqrt{T_n/T_o}$ are derived from equation (5). They are used in equation (6) to deduce the effective neutron temperatures. The second square bracket in equation (6) is determined from the activity ratio in the reference position where the neutron temperature is assumed equal to the physical temperature. Thus values of g_x, which is a known function of T_n, are derived from equation (6) and hence T_n values are determined. Combining the values of $r\sqrt{T_n/T_o}$ and T_n gives r.

4. Fast Fission Ratios

The fast fission ratio δ (the number of U-238 fissions per U-235 fission) was obtained by measuring the fission product gamma-ray activities in natural and depleted uranium metal foils.

The foils were the same diameter as the fuel pellets and were irradiated in a representative cross section of the central fuel assembly. The fission product gamma-counting rates, (above a threshold of 1.3 Mev) corrected for the U-235 fission in the depleted foil and the U-238 fissions in the natural foil, give the time dependent quantity

$$R_\gamma(t) = \left(\frac{\text{U-238 gamma-counting rate}}{\text{U-235 gamma-counting rate}}\right)_t \qquad (7)$$

The fast fission ratio is given by

$$\delta = P(t)\, R_\gamma(t) \qquad (8)$$

The time dependent calibration factor P(t) was found by irradiating the same foils in a fast neutron facility, where the fast fission ratio δ' was known, and counting the gamma-ray activities to obtain $R'_\gamma(t)$ and hence $P(t) = \delta'/R'_\gamma(t)$. A back-to-back fission chamber containing natural uranium on one side and U-235 on the other was used to obtain δ' by measuring the fission rate ratio, R', (natural U/U-235) with the chamber in the fast neutron facility and the corresponding ratio, R^o, with it in a thermal flux ($\delta = 0$). Then, $\delta' = (R'/R^o)-1$.

5. Initial Conversion Ratios

Values of the initial conversion ratio, γ_o (the number of Pu-239 atoms produced per U-235 atom destroyed) were determined by comparing the relative neptunium and relative fission product activities induced in thin wafers of natural uranium oxide in a representative cross section of the central fuel assembly and in

a thermal neutron flux either in a tank of D_2O attached to the end of a thermal column in the NRX reactor or in the ZED-2 bottom graphite reflector. The neptunium was counted using a coincidence method which suppresses the fission product and natural background rates ten times more than the neptunium rate. The details of this technique have been described by Tunnicliffe et al. (7) and Chidley et al. (8).

The conversion ratio is given in terms of the measured activity ratios by the following expression,

$$\gamma_o = C\left[\frac{\Sigma_a^{28}}{\Sigma_a^{25}}\right]_{\text{thermal}} \left[\frac{(1+\alpha)_{\text{thermal}}}{(1+\alpha)_{\text{fuel}}}\right]_{\text{U-235}} \qquad (9)$$

where Σ_a^{28}, Σ_a^{25} are the absorption cross sections of U-238 and U-235 respectively,

α is the ratio of capture to fission cross sections of U-235, and

$$C = \frac{\left[\frac{\text{Np-239 activity (fuel)}}{\text{Np-239 activity (thermal)}}\right]}{\left[\frac{\text{U-235 fission product activity (fuel)}}{\text{U-235 fission product activity (thermal)}}\right]} \qquad (10)$$

is the measured activity ratio corrected for U-238 fission product activity. Hence the absolute value of the initial conversion ratio γ_o is based on the value of $\left[\Sigma_a^{28}/\Sigma_a^{25}\right]_{\text{thermal}} = 0.562$ and values of $\frac{(1+\alpha)_{\text{thermal}}}{(1+\alpha)_{\text{fuel}}}$ obtained from reference (6) using the measured r-values and neutron temperatures. The correction for the U-238 fission product activity in fuel was the time dependent

quantity $R_\gamma(t)$ defined above, that is,

$$\text{(U-235 fission product activity)} = \frac{\text{(Observed fission product activity)}}{1 + R_\gamma(t)} \qquad (11)$$

Results and Discussion

The results of the buckling measurements are listed in Table II. The values given have been corrected for the loading effect of the experimental foils and thimbles and to the standard moderator conditions of 25°C and 99.63 atom % D_2O. The corrections were based on calculated temperature and purity coefficients obtained from POOOF, the latest version (due to Primeau (9)) of the Chalk River lattice calculation program. The errors quoted on the values of B^2_{Al} are based on the error calculated from the counting statistics and assumed foil positioning uncertainties or that given by the goodness-of-fit of the measured flux distributions to the assumed functions, whichever was the greater. The values quoted are the means of at least two (in one case six) individual measurements. The values of B^2_{ZR} have larger errors due to the uncertainty in the theory used to deduce $(B^2_{Al} - B^2_{ZR})$. B^2_{ZR} is $\sim$0.2 m^{-2} less than B^2_{Al} at the lowest pitch but this difference decreases to $\sim$ 0.1 m^{-2} at the widest lattice pitch studied. The differences observed are consistent with the differences in the cross sections of Al and zircaloy-2. The B^2_{Al} results are plotted in Fig. 4 as a function of lattice pitch. The curves shown in Fig. 4 are bucklings obtained with POOOF, the lattice calculation program.

Table II: Bucklings, Fast Fission Ratios and Initial Conversion Ratios

Coolant	Pitch	B^2_{Al} **	B^2_{ZR}	δ	γ_o
	cm	m^{-2}	m^{-2}		
D_2O	18	$1.407 \pm .047$	$1.19 \pm .07$	0.0564	0.9653
	19	$2.407 \pm .028$	-	-	-
	20	$2.995 \pm .034$	-	-	-
	21	$3.479 \pm .029$	$3.30 \pm .05$	0.0543	0.8660
	22	$3.804 \pm .024$	-	-	-
	24	$4.065 \pm .014$	$3.91 \pm .05$	0.0528	0.8037*
	26	$4.078 \pm .014$	-	-	-
	28	$3.952 \pm .013$	$3.80 \pm .03$	0.0481	0.7454
	30	$3.690 \pm .020$	-	-	-
	32	$3.380 \pm .010$	-	-	-
	34	$3.052 \pm .007$	-	-	-
	36	$2.754 \pm .012$	$2.64 \pm .03$	0.0475	0.7050
AIR	18	$0.718 \pm .086$	-	0.0659	0.9951
	20	$2.768 \pm .072$	-	-	-
	21	$3.351 \pm .055$	-	0.0623	0.8442
	22	$3.717 \pm .045$	-	-	-
	24	$4.115 \pm .036$	-	0.0565	0.7875
	26	$4.174 \pm .023$	-	-	-
	28	$4.070 \pm .018$	-	0.0549	0.7316
	30	$3.861 \pm .013$	-	-	-
	32	$3.576 \pm .022$	-	-	-
	34	$3.277 \pm .008$	-	-	-
	36	$2.970 \pm .006$	-	0.0532	0.6839
HB-40	18	$-0.365 \pm .062$	-	0.0581	0.9163
	21	$1.214 \pm .035$	-	0.0536	0.8266
	24	$1.568 \pm .019$	-	0.0521	0.7839
	28	$1.528 \pm .012$	-	0.0491	0.7575

* Average of two measurements.

**All buckling values correspond to moderator conditions of 25°C and 99.63 atom % D_2O.

As is evident from the graph, the calculations give bucklings lower than the measured values at large spacings and higher than the measured ones at small spacings. The program attempts to allow for the bundle end effects by assuming that the cluster materials are full-length but with effective areas consistent with the total volume of each material.

It should be mentioned here that there is a possible systematic error in the buckling results. Recent work by Henderson (10), who has applied the microscopic-discrete theory (11) to the calculation of flux distributions in lattices similar to those studied here, suggests that the effect of the flux transient at the core-reflector (or core-driver region) interface is not negligible at the outer points used in the present analysis to determine the radial bucklings. The results quoted here are derived using the five different radial positions shown in Fig. 3 to give the radial buckling; Henderson's analysis suggests that a more correct value is given by the three inner points. The effect is in a direction to give larger bucklings, and is more pronounced at tighter lattices. At the widest lattices the effect appears to be $\sim 0.05\ m^{-2}$ in B^2 but could be much larger at the closest spacings. Investigation of this effect is continuing. The effect could account for (at least partially) the discrepancy between the experiments and calculations at the smaller pitches.

The results of the microscopic neutron density distributions are listed in Table III, normalized to 1.000 in the fuel. It is to be noted that these results apply to the mid-bundle region, well-removed from the flux peaking effect at the end of the bundles.

Table III: Results of Microscopic Neutron Density Measurements

Coolant	Pitch cm	n_f*	n_s	n_c	n_{pt}	n_{ag}	n_{ct}	n_m
D_2O	18	1.000	1.033	1.162	1.431	1.440	1.452	1.685
	21	1.000	1.033	1.158	1.430	1.448	1.450	1.782
	24	1.000	1.021	1.147	1.427	1.454	1.467	1.856
	28	1.000	1.029	1.154	1.445	1.472	1.481	1.989
	32	1.000	1.032	1.147	1.452	1.479	1.489	2.087
	36	1.000	1.024	1.164	1.454	1.481	1.486	2.192
AIR	18	1.000	1.024	1.105	1.330	1.350	1.363	1.607
	21	1.000	1.023	1.090	1.330	1.350	1.358	1.713
	24	1.000	1.025	1.102	1.321	1.337	1.364	1.820
	28	1.000	1.033	1.110	1.333	1.363	1.409	1.946
	36	1.000	1.026	1.109	1.350	1.381	1.401	2.117
HB-40	18	1.000	1.048	1.195	1.650	1.701	1.713	1.863
	21	1.000	1.040	1.185	1.687	1.771	1.776	2.065
	24	1.000	1.034	1.195	1.763	1.796	1.806	2.109
	28	1.000	1.049	1.232	1.839	1.877	1.889	2.331
Flux Peaking Factors	21 (D_2O-cooled)	1.014	1.043	1.022	1.005	1.004	1.003	-

* Subscripts f, s, c, pt, ag, ct and m refer to fuel, sheath, coolant, pressure tube, air annulus, calandria tube and moderator, respectively.

In the 21 cm D_2O-cooled lattice a measurement was made of the flux peaking caused by the gap between the fuel in adjacent bundles. The results are given at the bottom of Table III as "flux peaking factors". The flux peaking factor for the i^{th} material is defined as the factor by which the mid-bundle neutron density in the i^{th} material must be multiplied to give the average (axial) neutron density in that material. It is assumed that the peaking factors are independent of lattice pitch and of type of coolant; the latter assumption is borne out by other experiments in lattices of 7-rod UO_2 bundles (2). The errors in the relative neutron densities are thought to be $\pm$ 2%. Throughout these measurements the moderator purity varied from 99.64 to 99.58 atom % and the temperature varied from 22°C to 28°C; no corrections have been made for these effects.

The measured values of r and T_n are given in Table IV. The temperatures are expressed as hardening values, ΔT, where ΔT_x is the difference between the neutron temperature at position x and the physical moderator temperature. We estimate the errors in r to be $\pm$ 3% (mainly due to the uncertainty in the In resonance parameters; the relative values of r are felt to be good to $\pm$ 1%) and in the ΔT values to be $\pm$ 3°C. (We believe that ΔT_m for the 24 cm air-cooled lattice is a flyer!) The values of $r\sqrt{T_n/T_o}$ and ΔT are plotted in Figs. 5 and 6 respectively against $V_{UO_2}/(V_{D_2O} + 3.753\ V_{HB\text{-}40})$ where V_{UO_2}, V_{D_2O} and $V_{HB\text{-}40}$ are volumes of UO_2, D_2O and HB-40 respectively per unit length of cell. The factor 3.753, equal to the ratio $(\xi\Sigma_s)_{HB\text{-}40}/(\xi\Sigma_s)_{D_2O}$ allows (at least nominally) for the greater moderating power of the HB-40.

Table IV: Neutron Spectrum Parameters

Coolant	Pitch	r_f*	r_m	r_s	ΔT_f**	ΔT_m	ΔT_s
	cm				°C	°C	°C
D_2O	18	0.0886	0.0626	0.0694	86	37	51
	21	0.0658	0.0428	0.0507	72	23	39
	24	0.0487	0.0309	0.0368	59	15	30
	28	0.0376	0.0226	0.0283	51	9	24
	36	0.0230	0.0120	0.0176	44	3	19
AIR	18	0.1001	0.0698	0.0805	86	43	64
	21	0.0720	0.0480	0.0585	72	25	47
	24	0.0535	0.0322	0.0418	63	28†	40
	28	0.0402	0.0244	0.0316	58	14	32
	36	0.0247	0.0128	0.0197	49	3	25
HB-40	18	0.0687	0.0451	0.0473	80	26	32
	21	0.0537	0.0317	0.0353	72	18	26
	24	0.0436	0.0242	0.0282	62	9	19
	28	0.0339	0.0176	0.0208	53	6	10

* Subscripts f, m, s refer to fuel average, a position in the moderator halfway between neighbouring rods, and the outer surface of the calandria tube, respectively.

** ΔT_x is the difference between the neutron temperature at position x and the physical moderator temperature.

† This value appears to be a flyer!

(V_{D_2O} includes both moderator and coolant in the D_2O-cooled cases.) The corresponding results for 7-element lattices are shown in Figs. 7 and 8. (Details of the 7-element fuel clusters are also listed in Table I.) In each figure, the upper values are for the cluster average and the lower values are for the cell boundary position in the moderator. The calandria tube values for the 19-element clusters which are not plotted, fall between the fuel and moderator values.

A linear dependence of $r\sqrt{T_n/T_o}$ and ΔT on $V_{UO_2}/(V_{D_2O} + 3.753\ V_{HB-40})$ is suggested and the straight lines shown as guides to the eye are the same in Figs. 5 and 7 and in Figs. 6 and 8. The cluster values of both $r\sqrt{T_n/T_o}$ and ΔT must approach a constant isolated rod value at wide spacings (small $V_{UO_2}/(V_{D_2O} + 3.753\ V_{HB-40})$) and this is suggested by the dashed extension of the lines although there is no indication of such curvature from the results. For the cell boundary results the lines through the $r\sqrt{T_n/T_o}$ values pass through the origin but the lines through the ΔT values have an intercept of about - 6^oC. This indicates a non-linearity at small values of ΔT or possibly an error in the assumption that the reference neutron temperature was equal to the moderator temperature.

These neutron spectrum parameters, when combined with the neutron density results listed in Table III, can be used to determine values of the thermal utilization f and thermal diffusion area L^2.

The experimental values of δ are listed in Table II and plotted in Fig. 9 against lattice pitch. Errors of $\pm$ 2% are indicated. An increase in δ with decreasing pitch is clearly

shown. The curves are of the form

$$\delta(d) = \delta(\infty)(1 + 6 \exp(-(d-2b)/\ell)) \qquad (12)$$

where $\delta(\infty)$ is the isolated cluster value,

d is the lattice pitch,

b = 1.5 cm is a constant, and

ℓ = 4.6 cm is the relaxation length for fission neutrons (causing fast fission) in D_2O (12). The exponential term is an approximation for the contribution from the six adjacent neighbours in the lattice. The values of $\delta(\infty)$ = 0.0476 and 0.0538 for D_2O coolant and air coolant respectively are indicated. The HB-40 values indicate $\delta(\infty)$ = 0.0480, not significantly higher than for D_2O.

The cluster average values of γ_o are listed in Table II. The values for D_2O-cooled lattices at spacings of 18, 21 and 28 cm are those given by Chidley et al. (8) but increased a small amount due to a reduction in the correction for the small gap ($\sim$ 0.013 mm) between the wafer and the pellets. This correction ($< 0.5\%$) was remeasured and found to be somewhat smaller than that used by Chidley et al. (8). New measurements of γ_o were made at 36 cm and 24 cm (two) and the values obtained are about 3% higher than those listed by Chidley et al. (8). The reason for this is not understood.

The values of γ_o have been plotted against $V_{UO_2}/(V_{D_2O} + 3.753\ V_{HB-40})$ in Fig. 10. An almost linear dependence, with an indication of curvature at large lattice spacings is suggested and curves have been drawn as guides to the eye.

The statistical counting errors, including uncertainties in the corrections, were in the range $\pm$ (0.3-0.5)%, that is, comparable with the size of the points in the figure. Measurements were made in all five elements across the cluster and consequently duplicate values of γ_o were obtained for the outer and inner rings of elements. The differences between these duplicate values are a measure of the consistency of the measurements. The root mean square difference for 27 pairs of γ_o values was 0.73% which corresponds to a 0.52% ($0.73/\sqrt{2}$) error for a single value. The corresponding average statistical error was about $\pm$ 0.4%. The larger rms deviation indicates an additional error of about $\pm$ 0.3%, perhaps due to misalignment of the wafers between pellets or misalignment of elements in the cluster. There is also the systematic error of $\pm$ 0.8% associated with the Maxwellian spectrum value (0.562) on which the results are based. More detailed discussion of the corrections and errors is given in references (7) and (8).

A comparison with the 7-element lattice values given by Tunnicliffe et al. (7) is made in Fig. 11 where the experimental points give the 7-element values and the curves the 19-element results. The trends are similar, with the 19-element values for each coolant about 3% higher than the 7-element values.

The values of δ and γ_o found here can be used in conjunction with the appropriate expressions to yield values for the fast fission factor ϵ, and the resonance escape probability p.

Summary

Experiments done in the critical facility ZED-2 to determine parameters for lattices of fuel assemblies which are a close mockup of the actual fuel channels of the power reactor CANDU (and also NPD) have been described.

The results of these measurements can now be compared with the same parameters obtained from the lattice recipes. The agreement between the measured and calculated parameters may then be useful as a guide to the development of better recipes. If the lattice recipes can predict correctly the results of clean, cold lattice experiments such as those described here, then some confidence can be felt in extrapolating them to the operating conditions appropriate to an actual power reactor.

Acknowledgements

The authors wish to acknowledge the help given by many people throughout the course of the work. In particular they would like to thank P.D.J. Ferrigan who was in charge of reactor operations; E. Engel, T.J. Manuel and J.T.R. Young who performed most of the experiments and also assisted with the analysis of the results; Mrs. M.G. Cahill who ran the data reduction and least squares computer programs an innumerable number of times; J.S. Rogers who helped with the analysis of the data and Miss E. Gehlert who typed the manuscript. D.B. Primeau kindly provided numerous POOOF calculations for the ZED-2 experimental conditions. Helpful discussions were held with B.G. Chidley, E. Critoph, W.J. Henderson, D.G. Hurst and A.G. Ward.

Bibliography

(1) G.A. Beer, D.W. Hone; "Lattice Measurements with 7-element UO_2 clusters in ZED-2, Part I: Bucklings Over a Range of Spacings with Three Coolants"; AECL-1505 (1962).

(2) R.E. Green, H. Markl, C.B. Bigham, A. Okazaki, J.W. Hilborn, E. Critoph; "Highlights of Chalk River Work on the Physics of Heavy Water Lattices Since the 1959 IAEA Panel Meeting"; AECL-1684 (1962).

(3) D.W. Hone, E. Critoph, M.F. Duret, R.E. Green, A. Okazaki, R.M. Pearce, L. Pease; "Natural Uranium Heavy-Water Lattices, Experiment and Theory"; Paper P/212, Proceedings of 2nd United Nations Conference on Atomic Energy, Geneva, 12, 351, (1958).

(4) C.H. Westcott, W.H. Walker, T.K. Alexander; "Effective Cross Sections and Cd Ratios for the Neutron Spectra of Thermal Reactors"; Paper P/202, Proceedings of 2nd United Nations Conference on Atomic Energy, Geneva, 16, 70, (1958).

(5) C.B. Bigham, B.G. Chidley, R.B. Turner; "Experimental Effective Cross Sections and Neutron Spectra in a Uranium Fuel Rod, Part II: CANDU-type Uranium Oxide Clusters"; AECL-1350 (1961).

(6) C.H. Westcott; "Effective Cross Section Values for Well Moderated Thermal Reactor Spectra"; AECL-1101 (1960).

(7) P.R. Tunnicliffe, D.J. Skillings, B.G. Chidley; "A Method For the Accurate Determination of Relative Initial Conversion Ratios"; Nuclear Science and Engineering, 15, 268 (1963).

(8) B.G. Chidley, T.J. Manuel, P.R. Tunnicliffe; "Initial Conversion Ratios and Fast Fission Factors in Heavy Water Natural Uranium Lattices Using 19-element UO_2 Fuel Rods". Nuclear Science and Engineering (In Press).

(9) D.B. Primeau; unpublished.

(10) W.J. Henderson, private communication.

(11) J.D. Stewart; "A Microscopic-Discrete Theory of Thermal Neutron Piles"; AECL-1470 (1962).

(12) C.B. Bigham, B.G. Chidley; AECL Progress Report PR-RRD-31, p. 70 (1962).

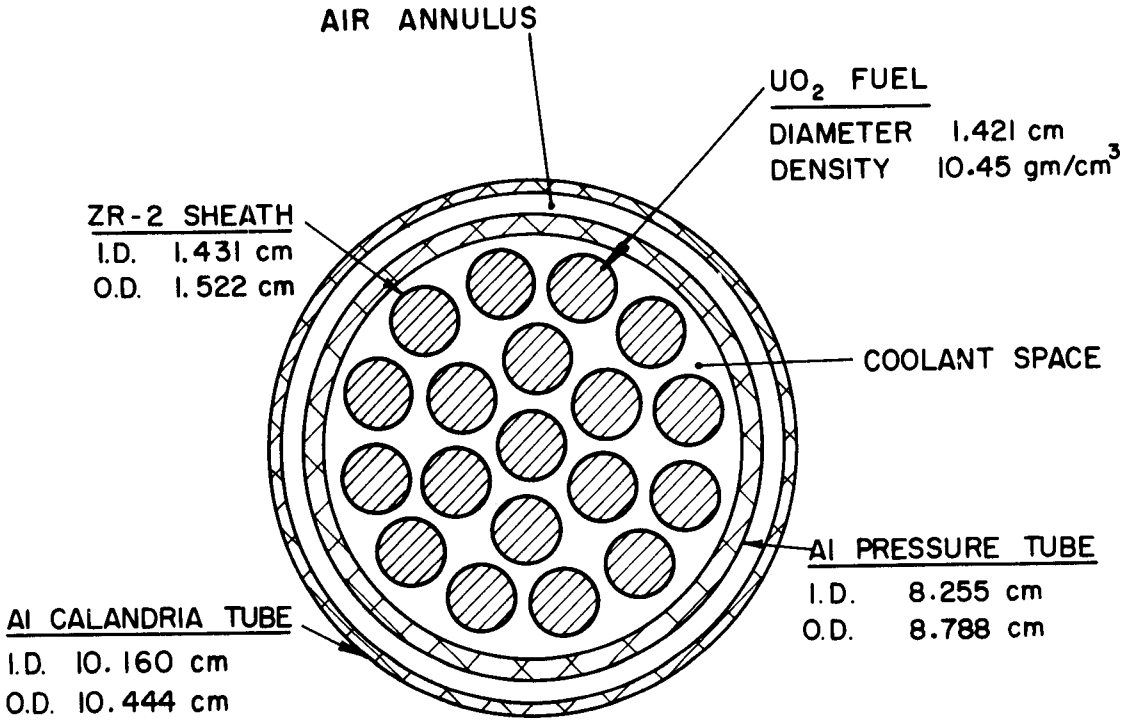

FIG. 1 CROSS SECTION OF
19-ROD FUEL ASSEMBLY

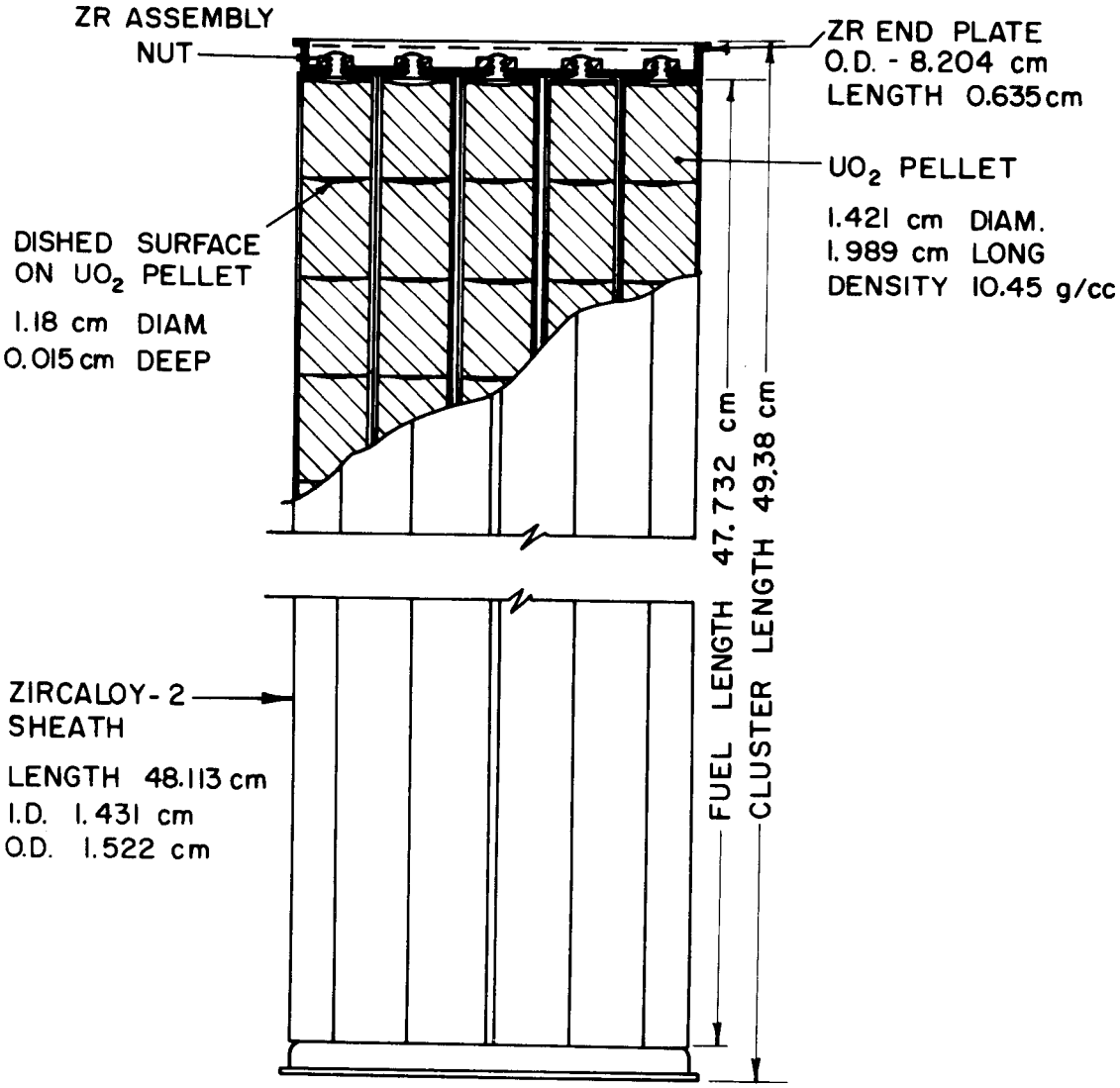

FIG. 2 DETAILS OF 19-ROD FUEL BUNDLE

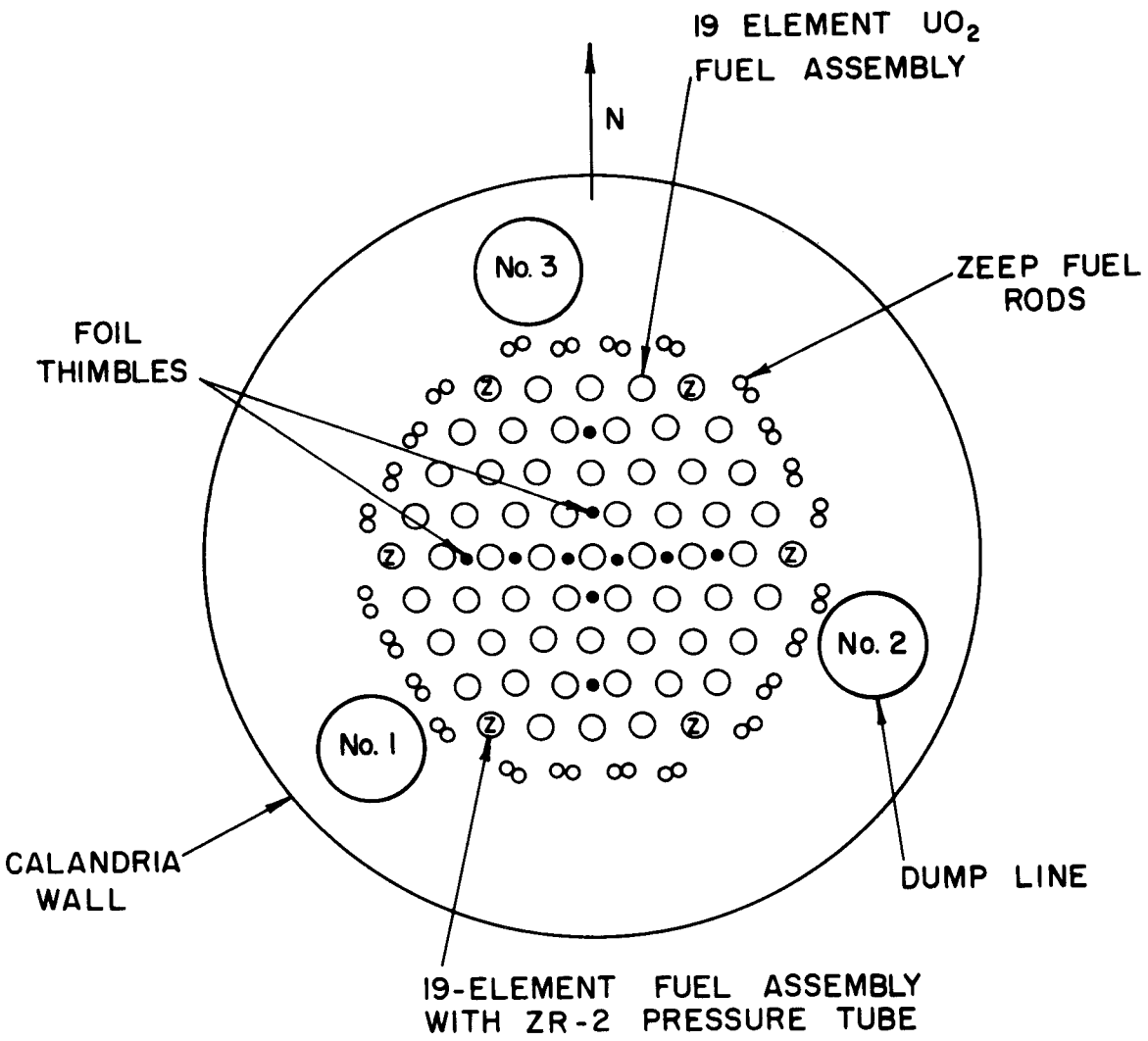

FIG. 3 21 cm D_2O-COOLED UO_2
(19) LATTICE

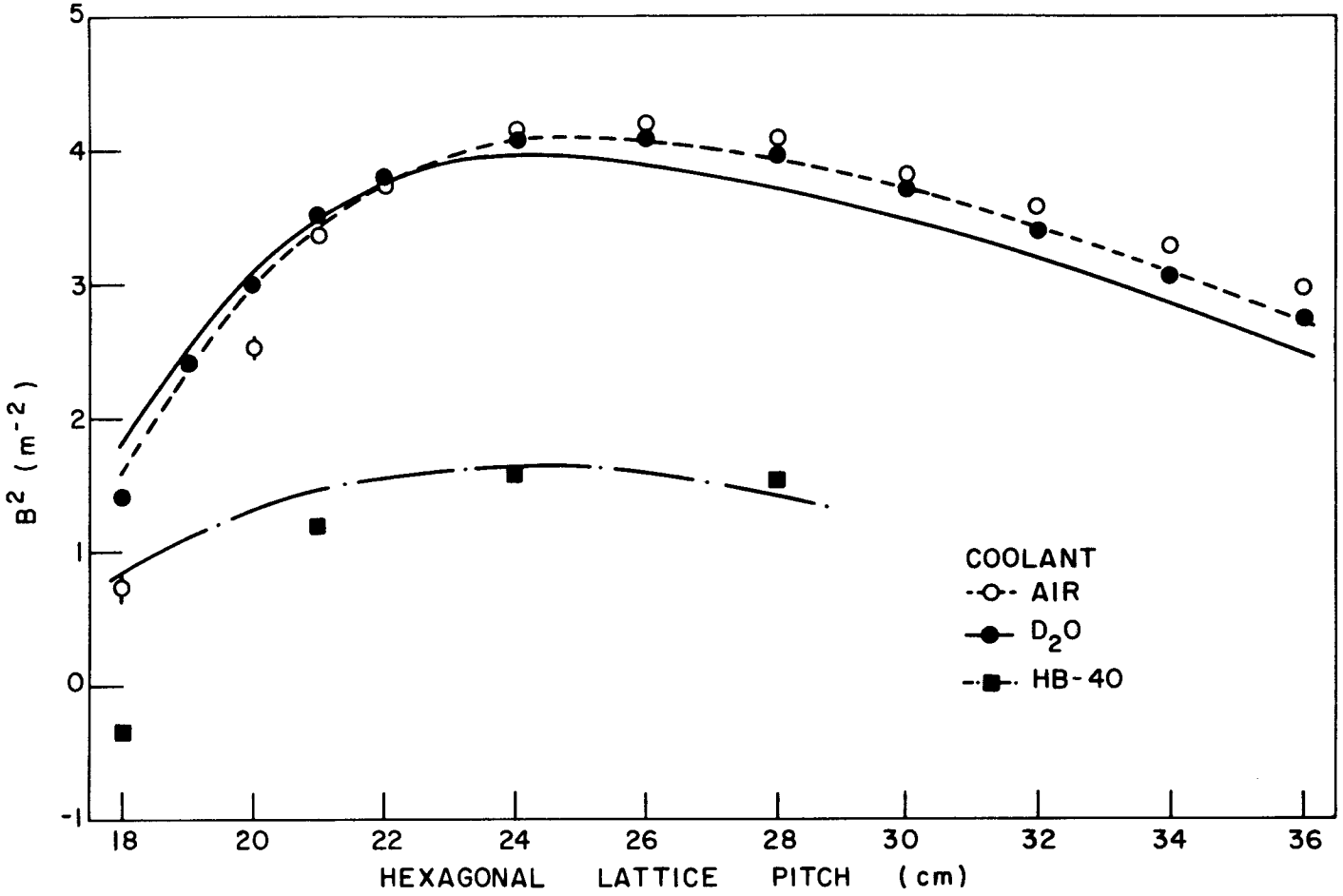

FIG. 4 BUCKLING vs LATTICE PITCH FOR CANDU TYPE FUEL ASSEMBLIES

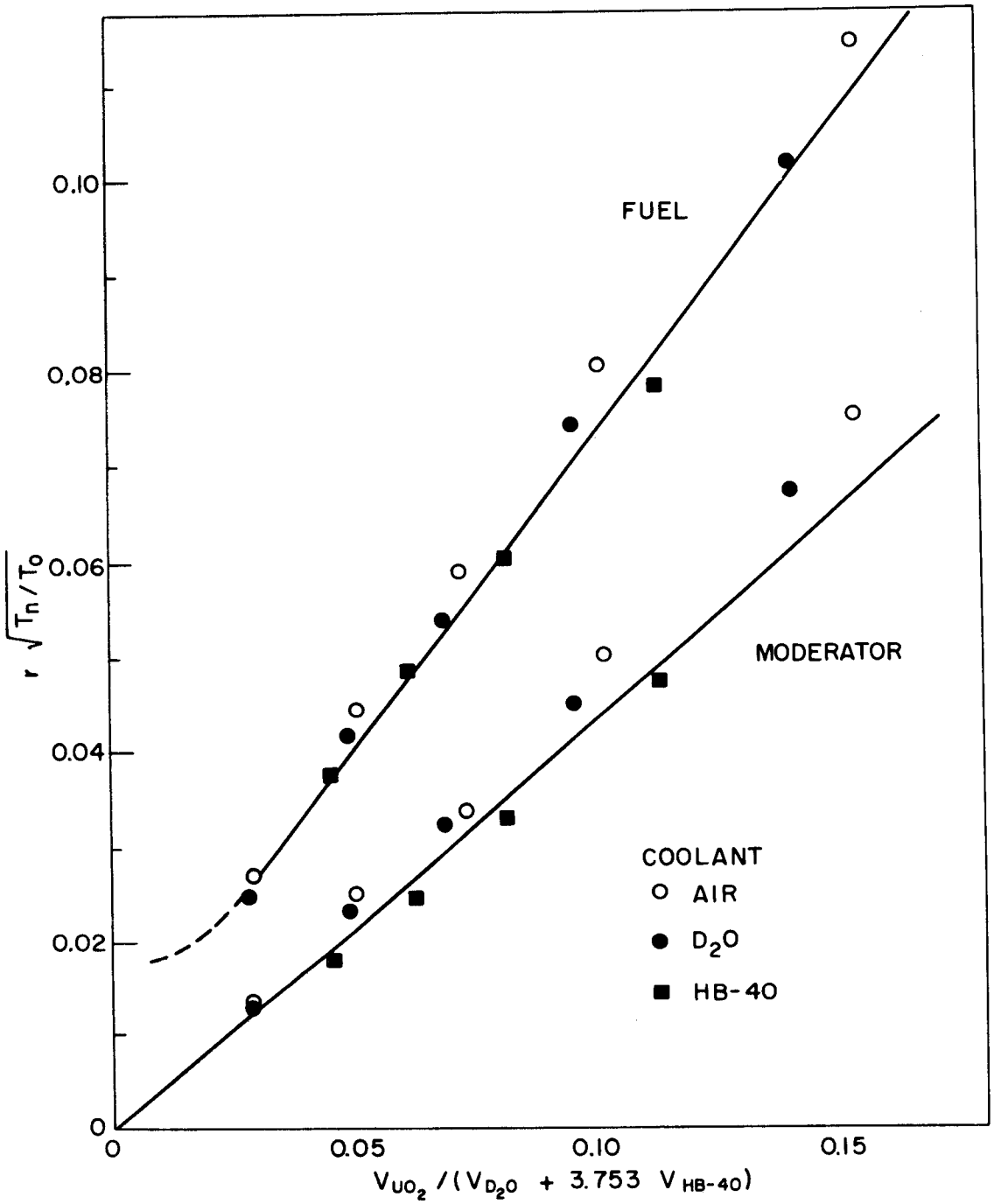

FIG. 5 $r\sqrt{T_n/T_0}$ VALUES IN 19-ELEMENT LATTICES

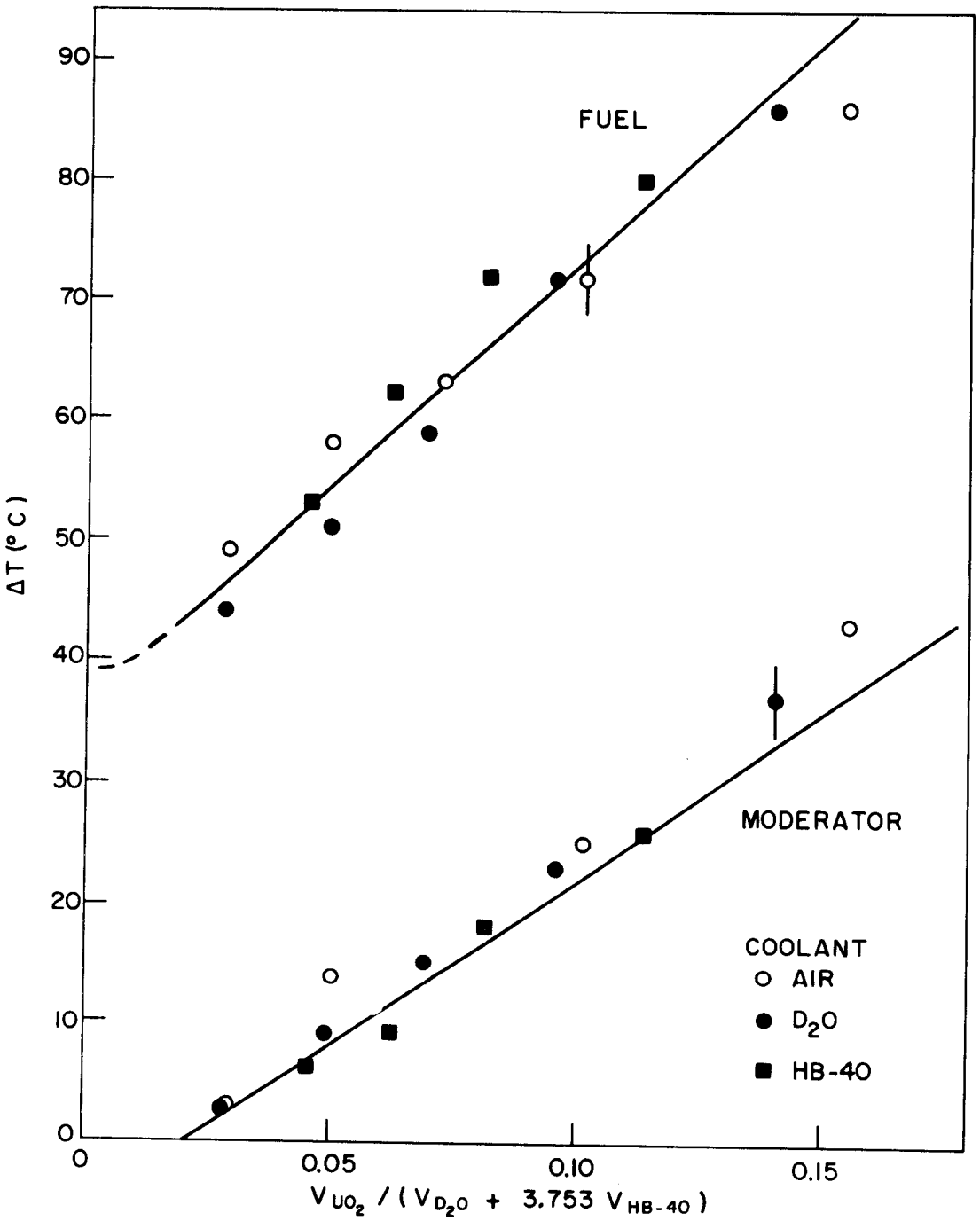

FIG. 6 ΔT_f AND ΔT_m VALUES IN 19-ELEMENT LATTICES

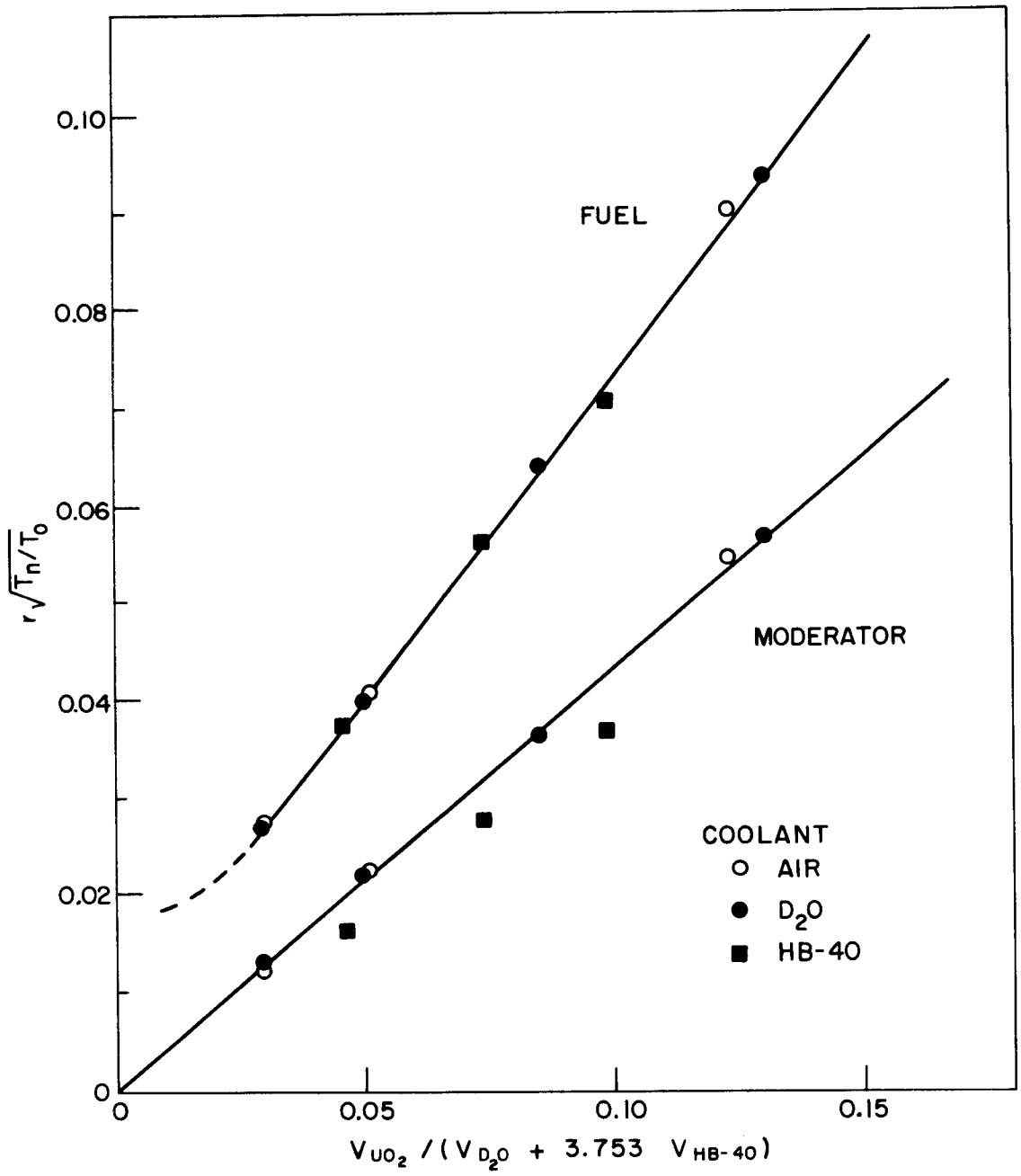

FIG. 7 $r\sqrt{T_n / T_0}$ VALUES IN 7-ELEMENT LATTICES

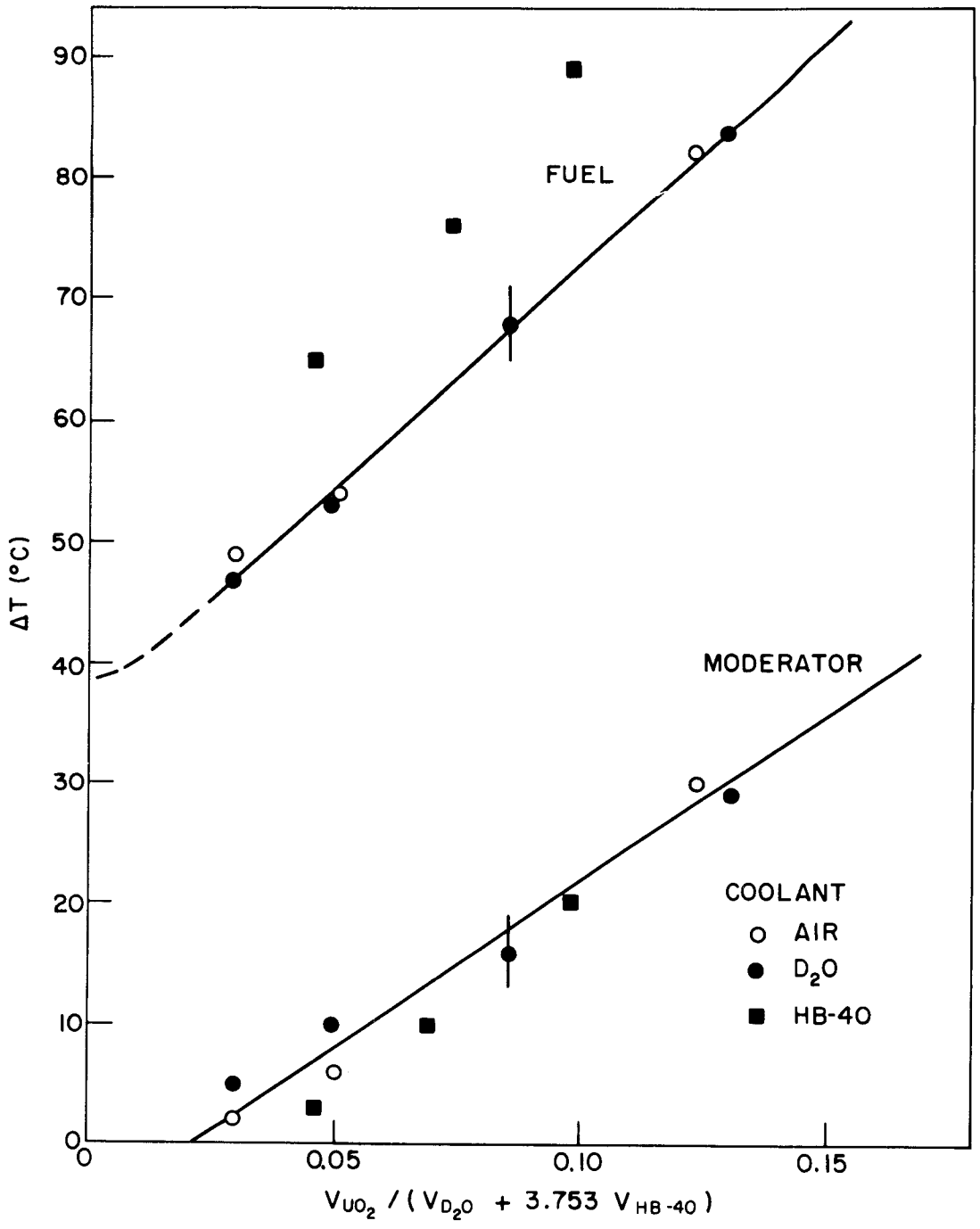

FIG. 8 ΔT_f AND ΔT_m VALUES IN 7-ELEMENT LATTICES

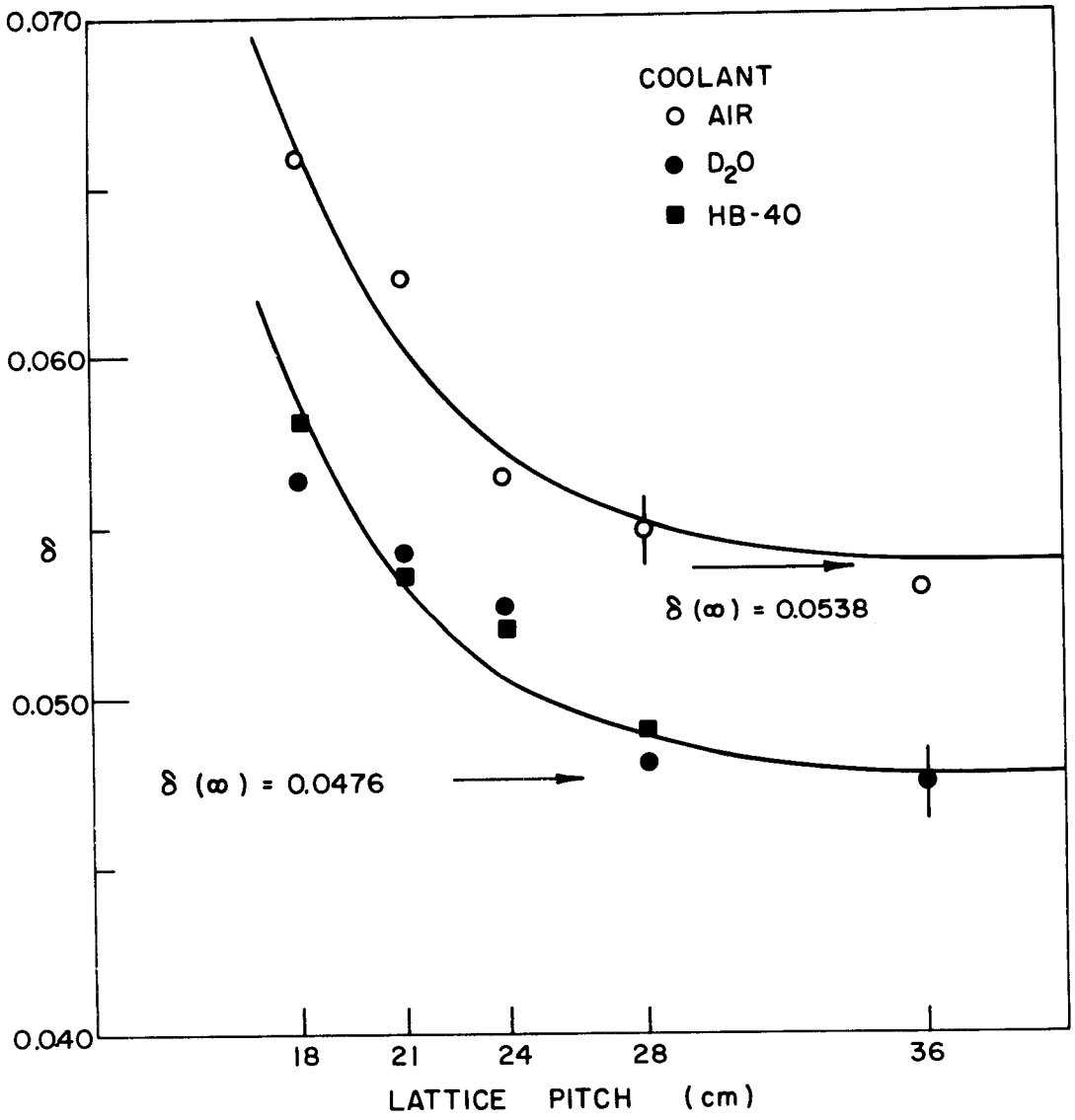

FIG. 9 FAST FISSION RATIOS IN 19-ELEMENT LATTICES

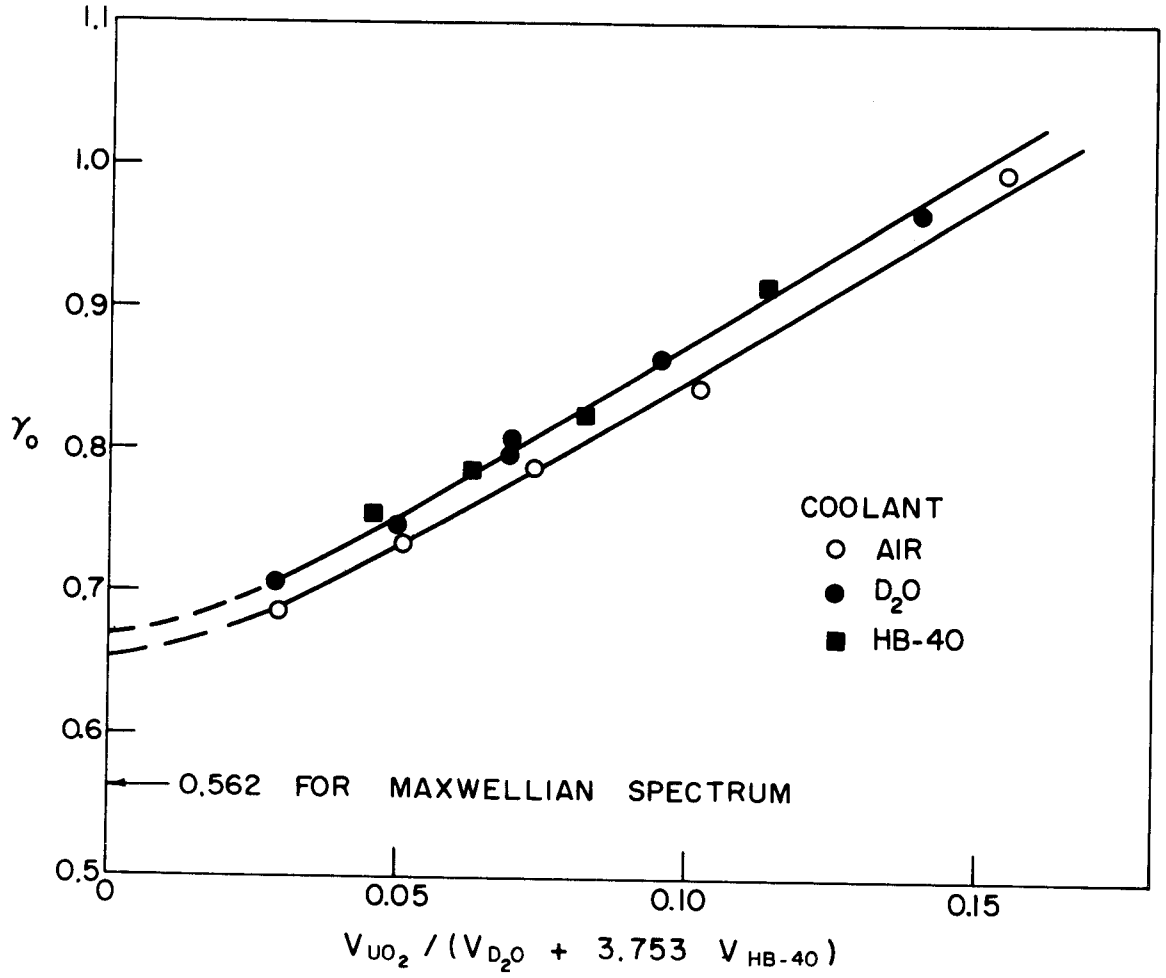

FIG. 10 INITIAL CONVERSION RATIOS IN 19-ELEMENT LATTICES

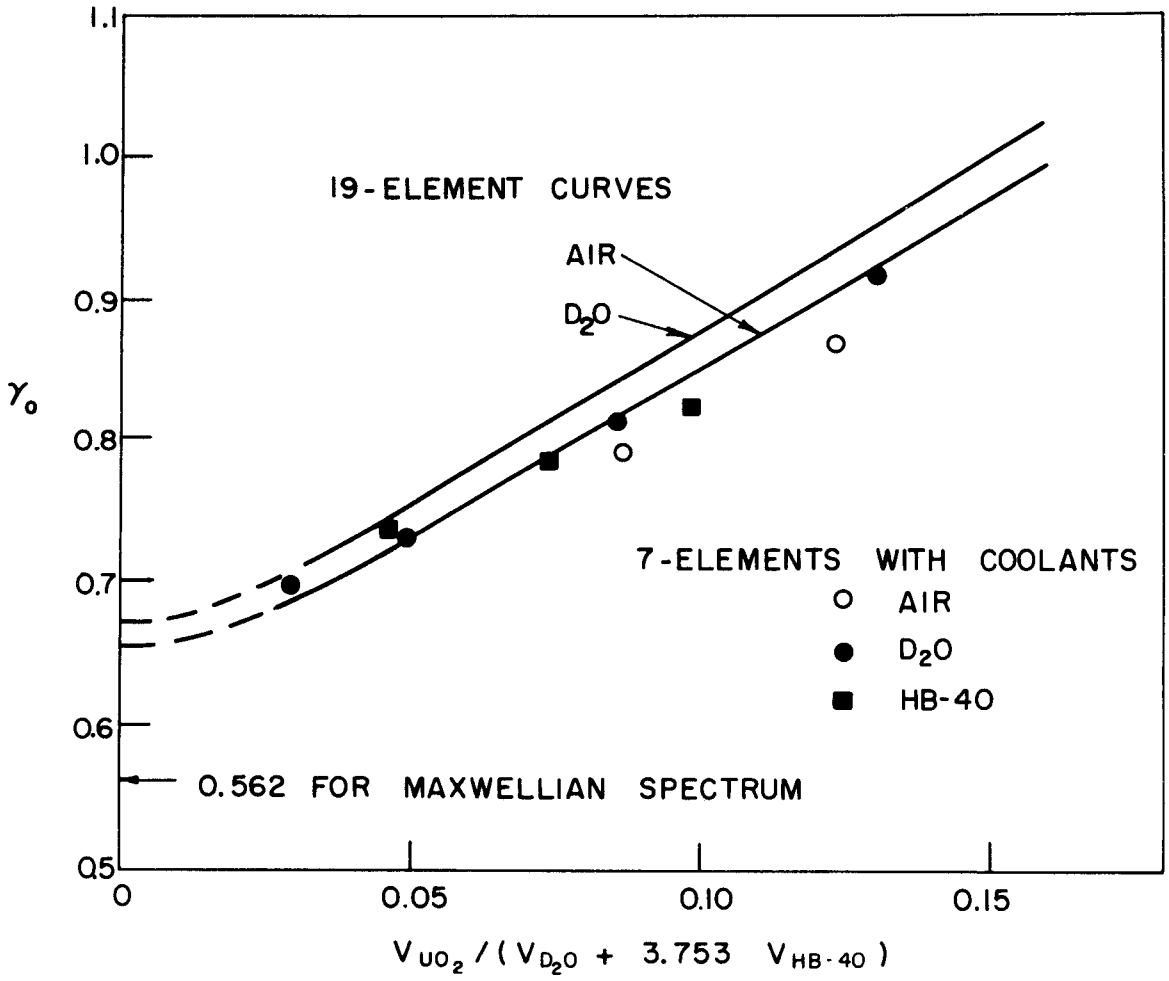

FIG. 11 INITIAL CONVERSION RATIOS IN 7 & 19 ELEMENT LATTICES